NASA Technical Memorandum 83058
AIAA-83-0135
0540

Validation of a Three-Dimensional Viscous Analysis of Axisymmetric Supersonic Inlet Flow Fields

T. J. Benson and B. H. Anderson
Lewis Research Center
Cleveland, Ohio

Prepared for the
Twenty-First Aerospace Sciences Conference
sponsored by the American Institute of
Aeronautics and Astronautics
Reno, Nevada, January 10–13, 1983

NASA

Validation of a Three-Dimensional Viscous Analysis of Axisymmetric Supersonic Inlet Flow Fields

by T. J. Benson and B. H. Anderson

National Aeronautics and Space Administration
Lewis Research Center
Cleveland, Ohio 44135

ABSTRACT

A three-dimensional viscous marching analysis for supersonic inlets has recently been developed. To verify this analysis several benchmark axisymmetric test configurations have been studied and are compared to experimental data. Detailed two-dimensional results for shock-boundary layer interactions are presented for flows with and without boundary layer bleed. Three-dimensional calculations of a cone at angle of attack and a full inlet at angle of attack are also discussed and evaluated. Results of the calculations demonstrate the code's ability to predict complex flow fields and establishes guidelines for future calculations using similar codes.

INTRODUCTION

Over the past few years, NASA Lewis Research Center has been increasingly involved in developing three-dimensional spatial marching analyses for the design of supersonic inlets. In support of this work, research was also initiated to systematically verify these computer analyses by a two tier verification process. The first tier involves establishing the ability of the computer analyses to predict flow parameters of interest in "generic" configurations which would be typical of real world designs. A second tier verification process was also initiated where the essential elements of the computer analyses are validated in very simple environments which highlight one or more basic or "benchmark" flow mechanisms. This is called "benchmark" verification of the computer code.

A thorough verification process for the PEPSIS computer code is being conducted at NASA Lewis. PEPSIS is a three-dimensional viscous marching analysis for supersonic inlets of axisymmetric, rectangular or conformal geometry which was jointly developed by Scientific Research Associates and NASA Lewis. Details of the algorithm and code development are given in (refs. 1 to 2). Some of the generic verification results have been presented in a paper by Anderson and Towne (ref. 3) and at the Lewis Computational Fluid Mechanics Workshop in 1980 (ref. 4). Anderson and Benson (ref. 5) present one of the benchmark results for rectangular geometry verification, while this paper presents results for axisymmetric geometries. Four major test cases will be considered in this study; the Lewis 40-60 inlet (ref. 6) at zero angle of attack, the two-dimensional shock-boundary layer interaction of Rose (ref. 7), the cone at angle of attack by Rainbird (ref. 8), and the Lewis 40-60 inlet at angle of attack.

ANALYSIS

PEPSIS, an acronym for Parabolic Elliptic Streamwise Implicit Supersonic, is a fully three-dimensional computer design code for supersonic inlets. The analysis retains the general three-dimensional viscous nature of the Navier-Stokes equations, but takes advantage of realistic physical approximations to limit computer run time and storage requirements associated with the solution of the full Navier-Stokes equations. The assumption is made that a primary flow direction exists and that diffusion arising from the rate of change of flow in this primary direction can be neglected. The resulting set of equations are solved by an efficient spatial marching procedure. The code can solve the three momentum equations, continuity equation, energy equation and turbulent kinetic energy equation simultaneously. The circumferential momentum equation is neglected for two-dimensional cases. For all of the calculations in this study, an assumed constant stagnation enthalpy has been substituted for the full energy equation, and a simple algebraic turbulence model of McDonald and Camarata (ref. 9) with Van Driest damping has been used instead of the one equation model.

In each of the test cases the effects of the number and location of radial, circumferential and streamwise mesh points has been studied. The effects of the mixing length scaling factor delta has also been studied in several of the test cases. Because of the many shock-boundary layer interactions present in inlet flow fields, it is quite difficult to determine the proper mixing length scaling. In this study, the scaling was assumed to be the average boundary layer height for the entire surface. On solid surfaces, the boundary conditions were zero normal velocity and either zero tangential velocity (no-slip) or a slip velocity determined by the law of the wall (wall function). On flow surfaces, the boundary conditions were determined by extrapolation from interior points along Mach lines which allows flow and shock waves to pass out of the computational domain. All lengths were non-dimensionalized by the cowl lip height.

Lewis Inlet 40-60

The first test case considered for PEPSIS verification was the Lewis 40-60 mixed compression inlet at zero degree angle of attack (ref. 6). The 40-60 inlet is a Mach 2.5 axisymmetric design with 40 percent of the total compression occuring upstream of the cowl and 60 percent internally. The inlet has a 12.5° half angle centerbody, cowl lip aligned with the inlet axis, and internal contouring to conduct the flow to the engine face.

The inlet compresses the flow through a system of shock waves. At the design Mach number, the shock generated by the centerbody passes just outside the cowl lip. A shock generated by the cowl reflects off the centerbody back onto the cowl and again back to the centerbody where the terminal shock is formed. To control boundary layer separation, bleed is provided at each of these shock reflection locations. Bleed is modeled in the calculations by specifying the mass flow through the surface at the appropriate locations; uniform bleed was specified, although the code allows for a distribution of bleed.

A two-dimensional calculation was made at design Mach number using an 89x360 mesh and Reynolds number of 51.0E6. Wall functions were applied to the centerbody and cowl surfaces and mesh points were moderately packed near these surfaces. A constant step size of 0.02 of the cowl lip height was specified

and the mixing length scale delta was set to 0.03 on the centerbody and 0.01 on the cowl. Figure 1 shows Mach number profiles and static pressure distributions on the cowl and centerbody. The Mach number profiles indicate that PEPSIS qualitatively predicts the proper shock formation and reflections. Quantitatively, the agreement with static pressure is quite good. The upper pressure plot shows a steady increase in pressure on the first part of the cowl due to contouring. Ahead of the shock reflection, 3.8 percent of the capture flow is bled which lowers the pressure both analytically and experimentally. The shock reflected from the centerbody then causes the pressure to rise rapidly. On the centerbody surface, lower curve, the pressure is constant up to the first shock impingement where the pressure increases. At this shock reflection, 0.28 percent of the capture flow is bled. Downstream, the pressure slowly increases due to the cowl contouring then sharply decreases as the flow passes the throat and starts to expand. Just downstream of the throat the reflected shock hits and the calculation ends. Figure 2 shows a comparison of analytical and experimental total pressure profiles with the experiment shown as symbols. The centerbody bleed occurs between the first two plot locations and the calculation does quite well both fore and aft of the bleed zone. Similar plots on the cowl in the high bleed region indicate that some refinement of the bleed model is required.

Figure 3 presents the results of varying some of the input parameters for the 40-60 inlet. In figure 3(a) an increase from 40 to 89 radial mesh points has provided better detail of the boundary layer structure aft of the first bleed zone. A case was also run with the streamwise step reduced from 0.02 to 0.005 which indicated little change in the profiles throughout the inlet. Figure 3(b) shows total pressure profiles for different values of mixing length scale delta. The figure indicates that the quantitative results are very sensitive to this parameter. An option to automatically determine this scaling within the code is being provided.

Rose Shock-Boundary Layer Interaction

While the Lewis 40-60 inlet test calculation gave accurate results fore and aft of an oblique shock-boundary layer interaction, further detailed verification of this interaction was required. The Lewis 40-60 inlet test was part of a parametric study of mixed compression inlet performance and data from this test was intended only for overall inlet system verification. Detailed shock-boundary layer benchmark experimental data was available from a study by Rose (ref. 7). His experiment consisted of a cone placed in a blow down circular tunnel at Mach 3.88. The shock generated by the cone intersected the tunnel boundary layer and reflected. The wall region was instrumented with static pressure taps and the boundary layer was measured extensively through the interaction.

A two-dimensional calculation was run on an 89x450 mesh with high mesh packing on the tunnel wall; there were approximately 30 mesh points in the boundary layer. The Mach number was set to 3.88 and the Reynolds number per foot was 50.0E6, mixing length scaling delta was 0.10. A boundary layer profile for the tunnel wall was required as part of the initial conditions. This starting profile was generated by a program from the analysis of Maise and McDonald (ref. 10) which is now incorporated in the code as an input option.

A comparison of the calculated and experimental wall static pressure distributions is shown in figure 4. The code correctly predicts the two stage pressure rise through the interaction; the first, rather abrupt rise with the incoming shock and the second, more gradual rise with the formation of the reflected shock wave. Figure 5 shows pitot pressure profiles through the interaction and a comparison with experimental values obtained with a traversing pitot probe. The incoming shock appears as a discontinuity in the experimental data, while the shock smearing of the analysis occurs over several grid points. Notice that the analysis very well predicts the thinning of the boundary layer through the interaction.

Rainbird Cone at Angle of Attack

To test the accuracy of the code for a full three-dimensional flow field, the flow about a cone at angle of attack was modeled. The experiment was conducted by Rainbird and consisted of a 12.5° half angle cone mounted in a wind tunnel which was run at various Mach numbers, Reynolds numbers and angles of attack. A single measuring station was located back along the cone and the cone was slowly rotated to obtain circumferential variations of pressure and velocity. Several different Mach number and angle of attack combinations were tested by the code; this study will present only results of the extreme Mach = 4.25, alpha = 15.6° case. While such extreme conditions will probably never be encountered by an axisymmetric mixed compression inlet, the ability to accurately calculate this case gives increased confidence in the accuracy of the code for much smaller angles of attack.

The flow in this case figure 6, forms a conical shock of varying strength; the windward side being stronger than the leeward. A pressure minimum develops about 30° from the leeward ray and an ever thickening boundary layer develops from the windward ray to this pressure minimum. Similarly, flow is drawn from the leeward ray towards the pressure minimum resulting in a thinner boundary layer on the leeward ray. The flow develops a recirculation vortex between the leeward ray and pressure minimum as the boundary layers from the windward and leeward side interact.

Several calculations for this case have been run; all of them at a Mach number of 4.25, Reynolds number per foot of 51.0E6., delta equal to 0.015, and streamwise step size varying from 0.002 to 0.02. Figure 6 shows the results of the last PEPSIS calculation for this case. The figure shows Mach number contours at a plane cutting through the axis of the cone. The conical shock is clearly visible as is the boundary layer structure along the cone surface. Qualitatively, the code correctly predicts the shock structure, the thickening boundary layer on the cone, the thinning of the boundary layer on the leeward side and the recirculation. Figure 7 shows details of this recirculation. The upper figure shows secondary velocity vectors and clearly indicates the recirculation in the s-shaped profiles near the top. Also evident are c-shaped profiles near the side which are also found experimentally. The lower figure shows Mach number contours in this region which again indicate a recirculation.

The calculation of figure 7 required an 80x50x220 (radial, circumferential, streamwise) mesh. The large number of mesh points were necessary to resolve all of the length scales for the important features of this flow problem; the creation of the conical shock, the movement of the shock away from the cone, the boundary layer and the recirculation region near the cone surface. Figure 8 demonstrates the importance of radial and circumferential mesh resolution for this problem. The figure shows Mach number contours for

the aft quadrant of the flow field for different meshes at a plane near the measuring station. All of the calculations required 220 streamwise stations, with nearly 100 of them located near the cone tip to resolve the formation of the shock. Figure 8(a) shows the results of the first calculation with 40 radial points packed near the cone surface and 19 circumferential points evenly spaced at every 10°. The results indicate a thickening of the boundary layer on the leeward side, and give no indication of a recirculation. Increasing the number of circumferential points to 37 evenly spaced at 5° while maintaing 40 radial points gives the results of figure 8(b). This calculation gives an indication of recirculation but with little detail. Because the recirculation is caused by interactions in the boundary layer, more resolution was required in the radial direction near the surface. Packing the 40 radial points closer to the surface, gave the results shown in figure 8(c). While resolving details of the surface, resolution of the shock wave was sacrificed which resulted in violent post shock pressure oscillations. To resolve both the shock and the boundary layer, the radial mesh was increased to 80 points. The results shown in figure 8(d) indicate that the calculation was then able to resolve boundary layer details without oscillations near the shock wave. Figure 8(e) shows one further refinement in which the circumferential mesh was increased to 50 points which were packed on both the windward and the leeward rays. The marked difference in the results of figure 8(a) and figure 8(e) clearly demonstrates the need to resolve all of the length scales present in this problem.

Figure 9 shows a quantitative comparison of circumferential static pressure distribution on the cone surface. The experimental values are given by the circles, while the results of a similarity analysis of Jones (ref. 11) are given by the squares. The comparison is very good, except near the windward ray, where the code underpredicts the pressure rise. There are several possible explanations for this discrepancy, including problems in the mixing length model near the plane of symmetry, errors in the mixing length scaling, or mesh resolution. A comparison of streamwise boundary layer profiles indicates that the calculated boundary layer thickness was too small for this test case. A thicker boundary layer would give a better agreement with experiment because the effective cone angle would be increased. The code does correctly model the pressure variations near the leeward ray.

Lewis 40-60 Inlet at Angle of Attack

One of the principal uses of the PEPSIS program will be the calculation of axisymmetric inlets at angle of attack. A verification test for this problem is presently planned at NASA Lewis using the 40-60 inlet. To demonstrate the code's ability to calculate inlets at angle of attack, the 40-60 inlet has been calculated at design Mach number at 2° angle of attack and at a Mach 3.0 overspeed at 2°. The design Mach number case failed due to subsonic flow on the leeward cowl at the first cowl reflection which qualitatively agrees with the results of an earlier wind tunnel test. The overspeed case was then calculated in order to better study the qualitative results of the code, and only results of this calculation are reported here.

For the inlet at design Mach number and at zero degrees angle of attack, the shock from the cone passes just off of the cowl lip. For the overspeed case, this shock is forced inside the cowl lip. At angle of attack, the shock translates forward on the leeward side and falls even farther inside on the windward side of the inlet creating a small expansion region on the cowl lip.

The calculation used a 49x19x480 mesh and wall function boundary conditions on solid surfaces. Considering the Rainbird results, boundary layer details for this rather coarse mesh are probably not resolved. However, the calculation does give the correct qualitative results for the inviscid part of the flow field. Figure 10 shows surface static pressure distribution on the cowl and cone. The shock waves are clearly shown as dark bands which are inclined relative to the inlet axis. On the cone, the shock system has moved forward on the leeward side and aft on the windward. On the cowl the first rather weak shock from the cone tip and the stronger shock from the cone reflection are evident. Also evident on the surface are pressure contours which are normal to the inlet axis, particularly near the throat section on the cone and along the cowl between shocks. These features are the results of compressions and expansions present in the inlet due to surface contouring. For another perspective, the plots of figure 11 show pressure and Mach number contours in the flow field at the windward, waterline, and leeward rays. On the windward ray, the cone shock falls inside the cowl; while on the leeward ray, the shock hits near the cowl lip. Pressure waves from the cowl contouring coalesce to strengthen the reflected shock more on the windward than the leeward. The reflected shock strikes the centerbody further forward on the leeward than the windward resulting in greater turning of the flow and a stronger shock on the leeward. For each shock reflection downstream of the throat, the leeward shock is stronger and has moved forward of the windward shock. Also evident are the expansions near the throat and its interaction with the shock system. Note that the expansion location is fixed geometrically while the shocks are not. The Mach number contours indicate this same behavior, but also shows the boundary layer variations through the calculation.

COMPUTING TIME

Because of the need to perform calculations on very large meshes, a premium is put on speed of the computer and the computer code. Table I documents the speed characteristics of the PEPSIS code on the NASA Lewis IBM 370 and CRAY I. There are two entries for the IBM 370 because the computer can be run in two basic modes; either debug, i.e., with an internal symbol dictionary (ISD), or in production (without ISD). The ISD imposes a performance penalty on the code which is documented in table I. The first two calculations were computed in the two-dimensional mode, and its speed advantage over the three-dimensional occurs as a result of keeping the whole problem in the core of the machine. The figures for the CRAY computer are estimates based on a seven to one speed increase over the IBM with ISD. A version of PEPSIS has been run on the CRAY to establish this ratio, although the version of the code used for this study has not yet been loaded on the CRAY at Lewis.

CONCLUSIONS

This paper has presented results from four test cases which are part of the verification effort for the three-dimensional supersonic inlet computer code PEPSIS. A two-dimensional calculation of the Lewis 40-60 axisymmetric mixed compression inlet indicated that the code qualitatively predicts the proper shock system formation. Wall static pressure distribution and boundary layer profiles fore and aft of a moderate bleed zone compared well with experimental results. The Rose test case verified the code's ability to quantitatively predict the details of an oblique shock-boundary layer interaction. The Rainbird test case of a 12.5° cone at angle of attack demonstrated the

code's ability to accurately model three-dimensional flow fields. The code has properly modeled the conical shock wave of varying strength, the cross flow boundary layer profiles and the leeward recirculation region. A large number of mesh points were required to resolve the details of all of these phenomenon; a mesh resolution study indicated that insufficient resolution gave either unstable or inaccurate results. Without a highly efficient, high speed code like PEPSIS, these detailed calculations would be impractical. The final test case involved the Lewis 40-60 inlet at 2° angle of attack. The results correctly model the three-dimensional shift of the shock system within axisymmetric inlets at angle of attack.

The calculation of supersonic inlet flow fields is an extremely complex problem because of the many flow phenomenon which occur. A typical axisymmetric inlet produces shock waves, expansions, boundary layers and their interaction with shock waves, and possible cross flow recirculations. For an accurate calculation, the computational mesh must resolve all of the length scales for all the phenomenon present in the flow. The Rainbird test case has illustrated possible problems associated with insufficient mesh resolution and indicated the magnitude of calculations which may be required for proper resolution.

In general, the PEPSIS code gave excellent results for the four test cases of this study. Although much work is planned to improve the fluid flow physics and decrease the computing time by conversion and optimization on the CRAY I computer, it is evident that the PEPSIS computer code is practical for three-dimensional supersonic inlet calculations.

REFERENCES

1. Buggeln, R.C., McDonald, H., Levy R., and Kreskovsky, J.P. "Development of a Three-Dimensional Supersonic Inlet Flow Analysis," NASA CR-3218, January, 1980.
2. Buggeln, R.C., McDonald H., and Kim, Y.N. "Computation of Multidimensional Viscous Supersonic Flow by Spatial Forward Marching," AIAA Paper No 83-0177, January 1983.
3. Anderson, B.H. and Towne, C.E., "Numerical Simulation of Supersonic Inlets Using a Three-Dimensional Viscous Flow Analysis," NASA TM-18411, January 1980.
4. Benson, T.J., "Application of Three Dimensional Viscous Marching Analysis to Supersonic Inlets," Advanced Computational Methods Workshop, NASA Lewis, November 1980.
5. Anderson, B.H., and Benson, T.J., "Numerical Solution to the Glancing Sidewall Oblique Shock Wave/Turbulent Boundary Layer Interaction in Three-Dimensions," AIAA Paper No 83-0136, January 1983.
6. Fukuda, M.K., Hingst, W.G., and Reshotko, E., "Control of Shock Wave-Boundary Layer Interactions by Bleed in Supersonic Mixed Compression Inlets," NASA CR-2595, August 1975.
7. Rose, W.C., "The Behavior of a Compressible Turbulent Boundary Layer in a Shock Wave Induced Adverse Pressure Gradient," PhD Thesis, University of Washington, 1972.
8. Rainbrd, W.J., "Turbulent Boundary Layer Growth and Separation on a Yawed Cone," AIAA Journal, December 1968, pp 2410,2416.
9. McDonald, H. and Camarata, F.J., "An Extended Mixing Length Approach for Computing the Turbulent Boundary Layer Development," Proceedings of Stanford Conference on Computation of Turbulent Boundary Layers Vol I, 1969, pp 83-98.

10. Maise, G. and McDonald, H., "Mixing Length and Kinematic Eddy Viscosity in a Compressible Boundary Layer," AIAA Journal, Vol 6, No 1, January 1968, pp 73–79.
11. Jones, D.J., "Numerical Solution of the Flow Field for Conical Bodies in a Supersonic Stream," NRCC Aeronautical Report LR 507, July 1968.

TABLE I - TEST CASES, MESH AND COMPUTING TIME

CASE	MESH	COMPUTING TIME (MIN)		
		IBM 370/3033		CRAY 1#
		ISD	NO ISD	
Lewis is 40-60 inlet at 0°	89x360 (32 040)	5.3	3.8	.7
Rose	89x450 (40 050)	6.6	4.7	.9
Rainbird	40x19x220 (167 200)	42.2	27.8	6.0
	80x50x220 (880 000)	----	144.4	31.7
Lewis 40-60 inlet at 0°	49x19x480 (446 880)	117.9	-----	16.8

#ESTIMATED TIME

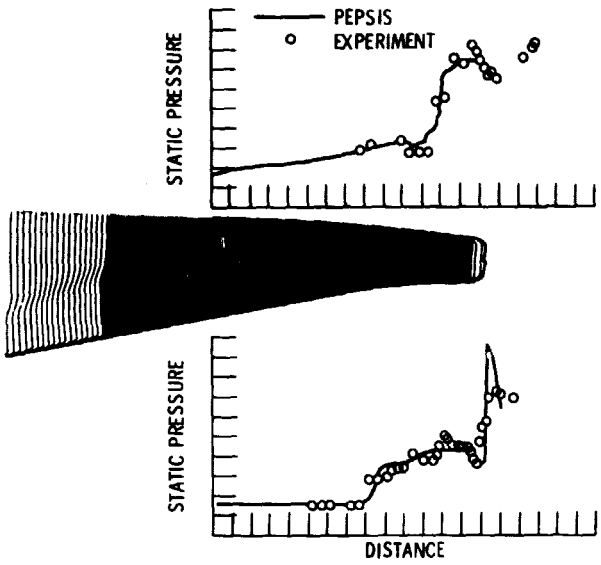

Figure 1. - Mach number profiles and wall static pressure distributions for Lewis 40-60 axisymmetric inlet.

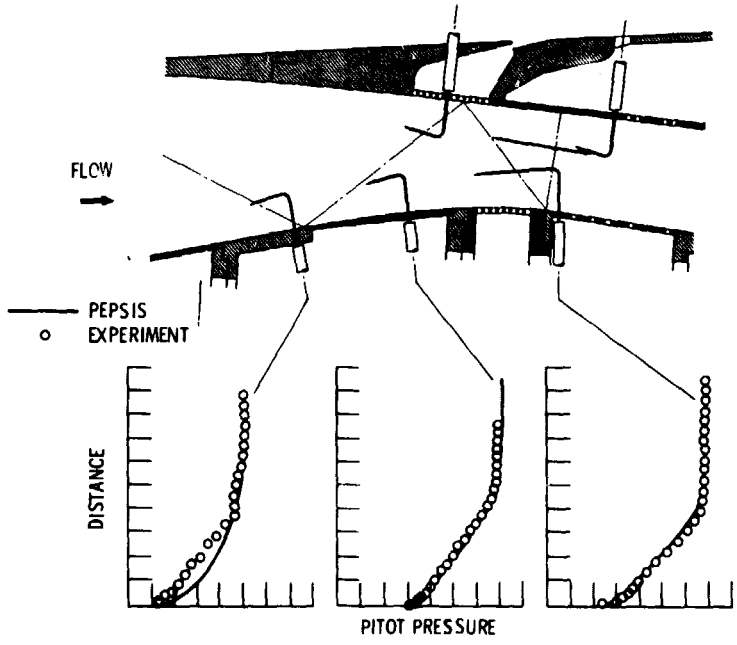

Figure 2. - Centerbody boundary layer profiles for Lewis 40-60 inlet.

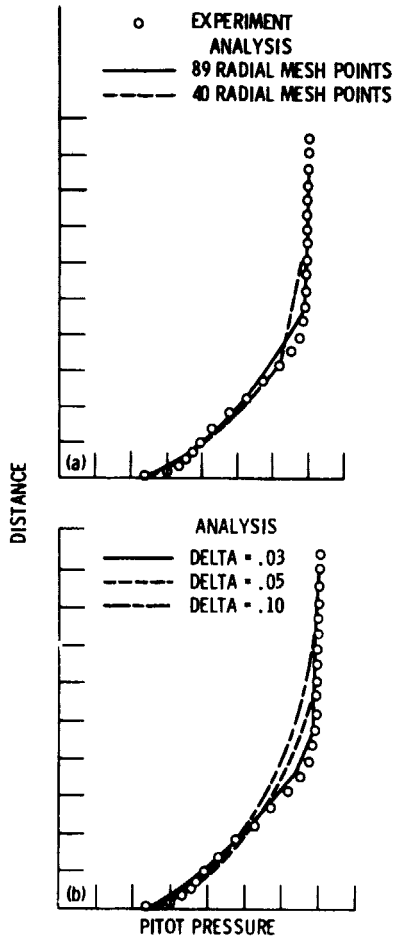

Figure 3. - Effects of input parameters on Lewis 40-60 inlet boundary layer profiles at rake 2.

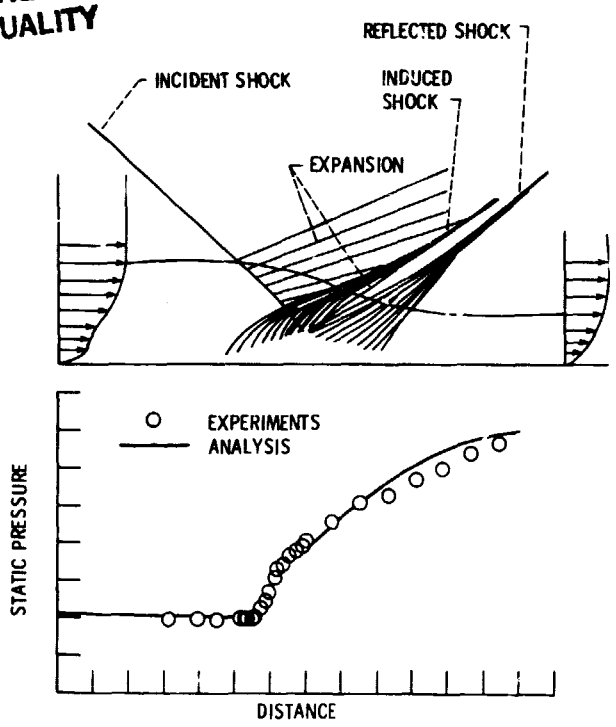

Figure 4. - Tunnel wall static pressure distribution for Rose shock-boundary layer interaction.

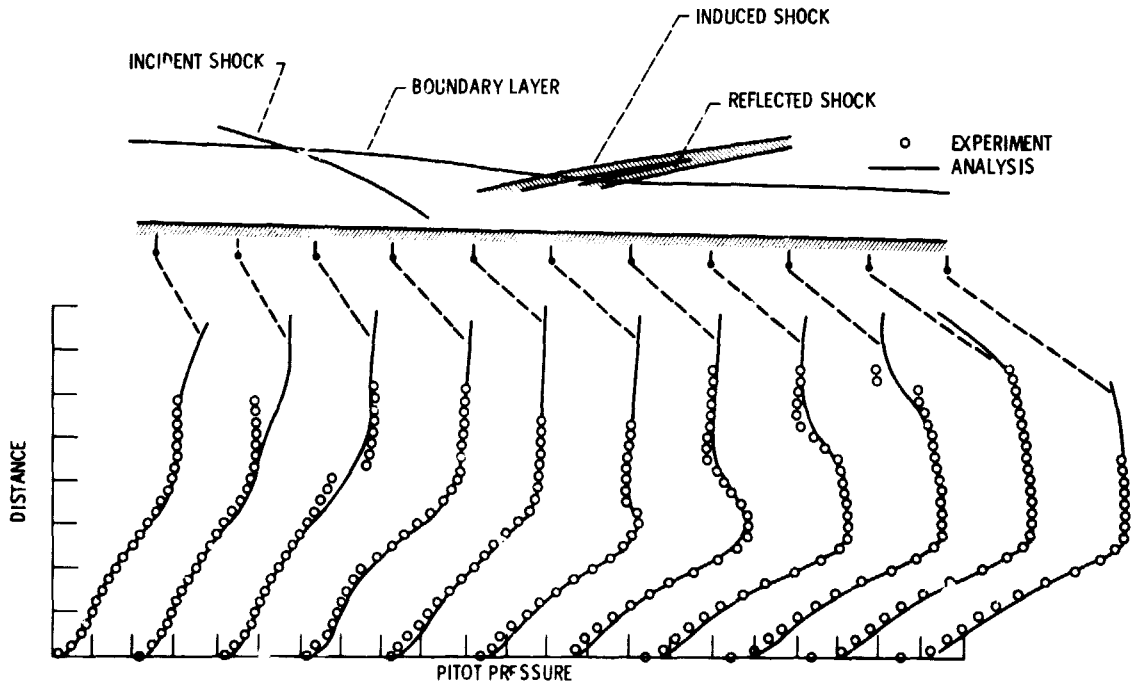

Figure 5. - Pitot pressure profiles for Rose shock-boundary layer interaction.

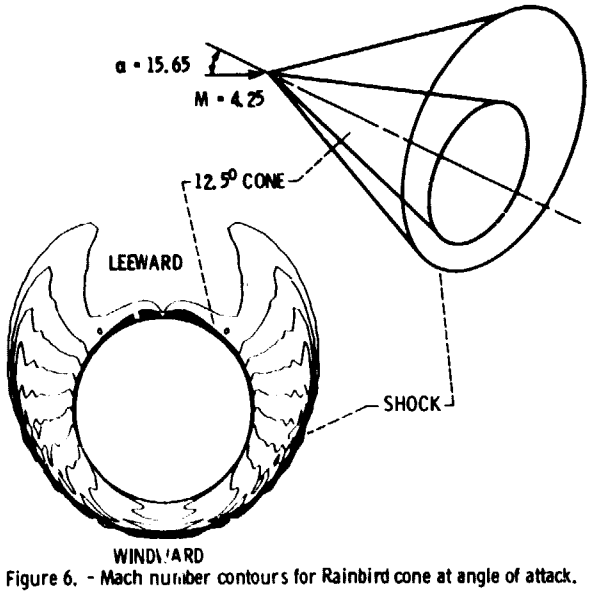

Figure 6. - Mach number contours for Rainbird cone at angle of attack.

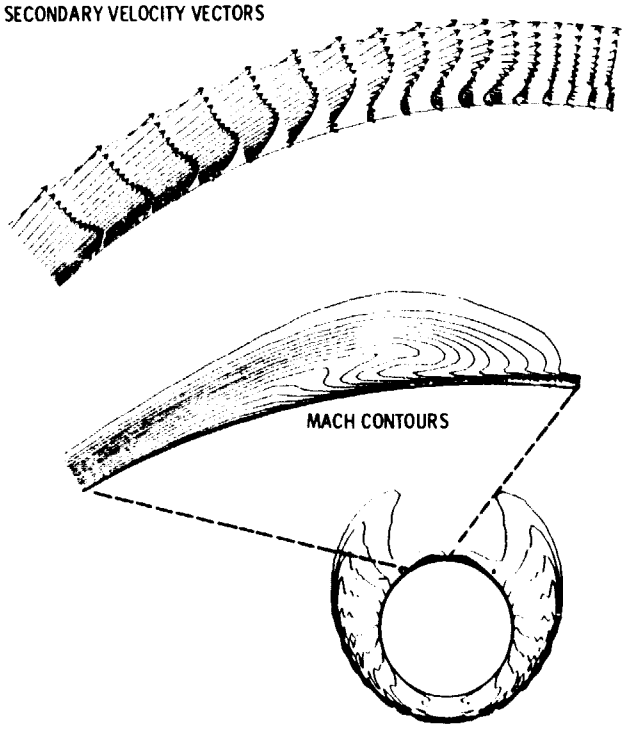

Figure 7. - Details of recirculation for Rainbird cone at angle of attack.

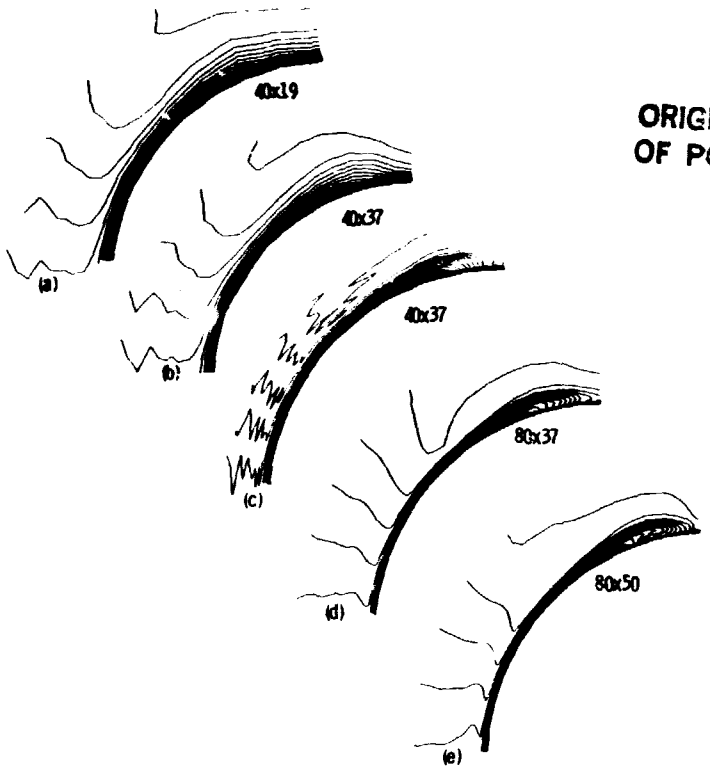

Figure 3. - Effects of mesh resolution on Rainbird cone at angle of attack.

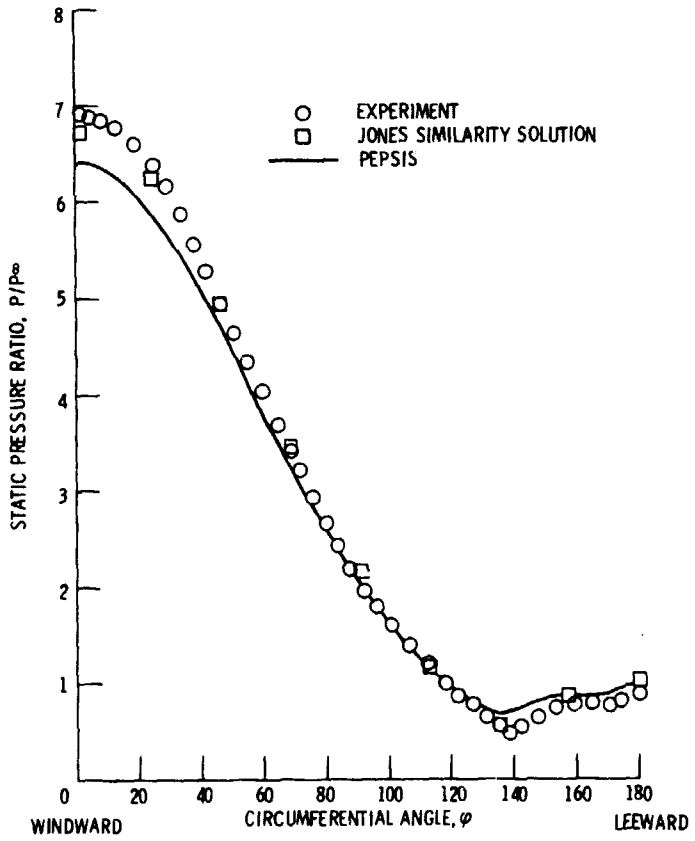

Figure 9. - Circumferential pressure distribution for Rainbird cone at angle of attack.

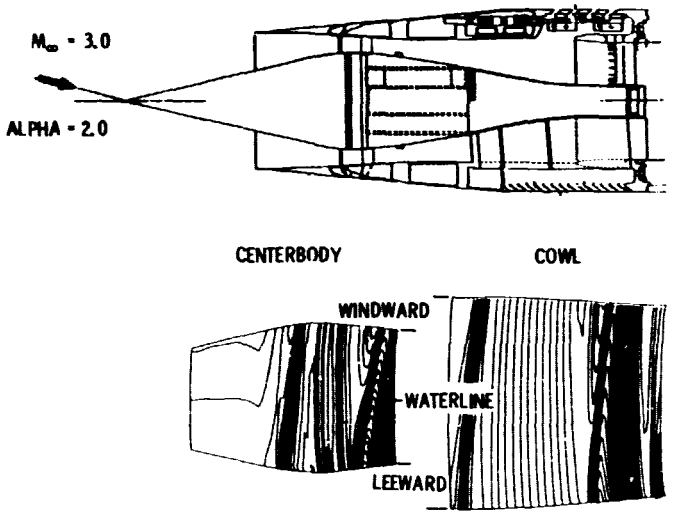

Figure 10. - Centerbody and cowl surface static pressure distribution for Lewis 40-60 inlet at angle of attack.

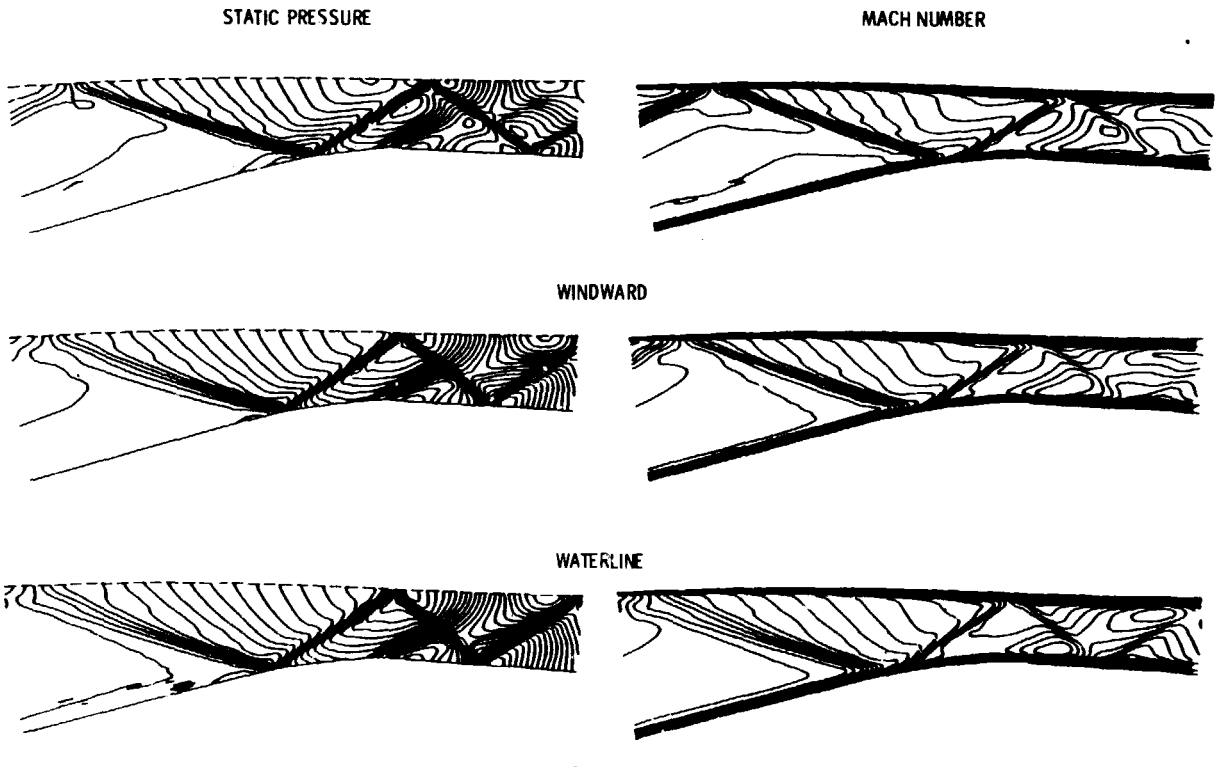

Figure 11. - Static pressure and Mach number contours for Lewis 40-60 inlet at angle of attack.

Validation of a Three-Dimensional Viscous Analysis of Axisymmetric Supersonic Inlet Flow Fields

T. J. Benson and R. H. Anderson
Lewis Research Center
Cleveland, Ohio

Prepared for the
Twenty-First Aerospace Sciences Conference
sponsored by the American Institute of
Aeronautics and Astronautics
Reno, Nevada, January 10–13, 1983

NASA

Validation of a Three-Dimensional Viscous Analysis of Axisymmetric Supersonic Inlet Flow Fields

by T. J. Benson and B. H. Anderson

National Aeronautics and Space Administration
Lewis Research Center
Cleveland, Ohio 44135

ABSTRACT

A three-dimensional viscous marching analysis for supersonic inlets has recently been developed. To verify this analysis several benchmark axisymmetric test configurations have been studied and are compared to experimental data. Detailed two-dimensional results for shock-boundary layer interactions are presented for flows with and without boundary layer bleed. Three-dimensional calculations of a cone at angle of attack and a full inlet at angle of attack are also discussed and evaluated. Results of the calculations demonstrate the code's ability to predict complex flow fields and establishes guidelines for future calculations using similar codes.

INTRODUCTION

Over the past few years, NASA Lewis Research Center has been increasingly involved in developing three-dimensional spatial marching analyses for the design of supersonic inlets. In support of this work, research was also initiated to systematically verify these computer analyses by a two tier verification process. The first tier involves establishing the ability of the computer analyses to predict flow parameters of interest in "generic" configurations which would be typical of real world designs. A second tier verification process was also initiated where the essential elements of the computer analyses are validated in very simple environments which highlight one or more basic or "benchmark" flow mechanisms. This is called "benchmark" verification of the computer code.

A thorough verification process for the PEPSIS computer code is being conducted at NASA Lewis. PEPSIS is a three-dimensional viscous marching analysis for supersonic inlets of axisymmetric, rectangular or conformal geometry which was jointly developed by Scientific Research Associates and NASA Lewis. Details of the algorithmn and code development are given in (refs. 1 to 2). Some of the generic verification results have been presented in a paper by Anderson and Towne (ref. 3) and at the Lewis Computational Fluid Mechanics Workshop in 1980 (ref. 4). Anderson and Benson (ref. 5) present some of the benchmark results for rectangular geometry verification, while this paper presents results for axisymmetric geometries. Four major test cases will be considered in this study; the Lewis 40-60 inlet (ref. 6) at zero angle of attack, the two-dimensional shock-boundary layer interaction of Rose (ref. 7), the cone at angle of attack by Rainbird (ref. 8), and the Lewis 40-60 inlet at angle of attack.

ANALYSIS

PEPSIS, an acronym for Parabolic Elliptic Streamwise Implicit Supersonic, is a fully three-dimensional computer design code for supersonic inlets. The analysis retains the general three-dimensional viscous nature of the Navier-Stokes equations, but takes advantage of realistic physical approximations to limit computer run time and storage requirements associated with the solution of the full Navier-Stokes equations. The assumption is made that a primary flow direction exists and that diffusion arising from the rate of change of flow in this primary direction can be neglected. The resulting set of equations are solved by an efficient spatial marching procedure. The code can solve the three momentum equations, continuity equation, energy equation and turbulent kinetic energy equation simultaneously. The circumferential momentum equation is neglected for two-dimensional cases. For all of the calculations in this study, an assumed constant stagnation enthalpy has been substituted for the full energy equation, and a simple algebraic turbulence model of McDonald and Camarata (ref. 9) with Van Driest damping has been used instead of the one equation model.

In each of the test cases the effects of the number and location of radial, circumferential and streamwise mesh points has been studied. The effects of the mixing length scaling factor delta has also been studied in several of the test cases. Because of the many shock-boundary layer interactions present in inlet flow fields, it is quite difficult to determine the proper mixing length scaling. In this study, the scaling was assumed to be the average boundary layer height for the entire surface. On solid surfaces, the boundary conditions were zero normal velocity and either zero tangential velocity (no-slip) or a slip velocity determined by the law of the wall (wall function). On flow surfaces, the boundary conditions were determined by extrapolation from interior points along Mach lines which allows flow and shock waves to pass out of the computational domain. All lengths were nondimensionalized by the cowl lip height.

Lewis Inlet 40-60

The first test case considered for PEPSIS verification was the Lewis 40-60 mixed compression inlet at zero degree angle of attack (ref. 6). The 40-60 inlet is a Mach 2.5 axisymmetric design with 40 percent of the total compression occuring upstream of the cowl and 60 percent internally. The inlet has a 12.5° half angle centerbody, cowl lip aligned with the inlet axis, and internal contouring to conduct the flow to the engine face.

The inlet compresses the flow through a system of shock waves. At the design Mach number, the shock generated by the centerbody passes just outside the cowl lip. A shock generated by the cowl reflects off the centerbody back onto the cowl and again back to the centerbody where the terminal shock is formed. To control boundary layer separation, bleed is provided at each of these shock reflection locations. Bleed is modeled in the calculations by specifying the mass flow through the surface at the appropriate locations; uniform bleed was specified, although the code allows for a distribution of bleed.

A two-dimensional calculation was made at design Mach number using an 89x360 mesh and Reynolds number of 51.0E6. Wall functions were applied to the centerbody and cowl surfaces and mesh points were moderately packed near these surfaces. A constant step size of 0.02 of the cowl lip height was specified

and the mixing length scale delta was set to 0.03 on the centerbody and 0.01 on the cowl. Figure 1 shows Mach number profiles and static pressure distributions on the cowl and centerbody. The Mach number profiles indicate that PEPSIS qualitatively predicts the proper shock formation and reflections. Quantitatively, the agreement with static pressure is quite good. The upper pressure plot shows a steady increase in pressure on the first part of the cowl due to contouring. Ahead of the shock reflection, 3.8 percent of the capture flow is bled which lowers the pressure both analytically and experimentally. The shock reflected from the centerbody then causes the pressure to rise rapidly. On the centerbody surface, lower curve, the pressure is constant up to the first shock impingement where the pressure increases. At this shock reflection, 0.28 percent of the capture flow is bled. Downstream, the pressure slowly increases due to the cowl contouring then sharply decreases as the flow passes the throat and starts to expand. Just downstream of the throat the reflected shock hits and the calculation ends. Figure 2 shows a comparison of analytical and experimental total pressure profiles with the experiment shown as symbols. The centerbody bleed occurs between the first two plot locations and the calculation does quite well both fore and aft of the bleed zone. Similar plots on the cowl in the high bleed region indicate that some refinement of the bleed model is required.

Figure 3 presents the results of varying some of the input parameters for the 40-60 inlet. In figure 3(a) an increase from 40 to 89 radial mesh points has provided better detail of the boundary layer structure aft of the first bleed zone. A case was also run with the streamwise step reduced from 0.02 to 0.005 which indicated little change in the profiles throughout the inlet. Figure 3(b) shows total pressure profiles for different values of mixing length scale delta. The figure indicates that the quantitative results are very sensitive to this parameter. An option to automatically determine this scaling within the code is being provided.

Rose Shock-Boundary Layer Interaction

While the Lewis 40-60 inlet test calculation gave accurate results fore and aft of an oblique shock-boundary layer interaction, further detailed verification of this interaction was required. The Lewis 40-60 inlet test was part of a parametric study of mixed compression inlet performance and data from this test was intended only for overall inlet system verification. Detailed shock-boundary layer benchmark experimental data was available from a study by Rose (ref. 7). His experiment consisted of a cone placed in a blow down circular tunnel at Mach 3.88. The shock generated by the cone intersected the tunnel boundary layer and reflected. The wall region was instrumented with static pressure taps and the boundary layer was measured extensively through the interaction.

A two-dimensional calculation was run on an 89x450 mesh with high mesh packing on the tunnel wall; there were approximately 30 mesh points in the boundary layer. The Mach number was set to 3.88 and the Reynolds number per foot was 50.0E6, mixing length scaling delta was 0.10. A boundary layer profile for the tunnel wall was required as part of the initial conditions. This starting profile was generated by a program from the analysis of Maise and McDonald (ref. 10) which is now incorporated in the code as an input option.

A comparison of the calculated and experimental wall static pressure distributions is shown in figure 4. The code correctly predicts the two stage pressure rise through the interaction; the first, rather abrupt rise with the incoming shock and the second, more gradual rise with the formation of the reflected shock wave. Figure 5 shows pitot pressure profiles through the interaction and a comparison with experimental values obtained with a traversing pitot probe. The incoming shock appears as a discontinuity in the experimental data, while the shock smearing of the analysis occurs over several grid points. Notice that the analysis very well predicts the thinning of the boundary layer through the interaction.

Rainbird Cone at Angle of Attack

To test the accuracy of the code for a full three-dimensional flow field, the flow about a cone at angle of attack was modeled. The experiment was conducted by Rainbird and consisted of a 12.5° half angle cone mounted in a wind tunnel which was run at various Mach numbers, Reynolds numbers and angles of attack. A single measuring station was located back along the cone and the cone was slowly rotated to obtain circumferential variations of pressure and velocity. Several different Mach number and angle of attack combinations were tested by the code; this study will present only results of the extreme Mach = 4.25, alpha = 15.6° case. While such extreme conditions will probably never be encountered by an axisymmetric mixed compression inlet, the ability to accurately calculate this case gives increased confidence in the accuracy of the code for much smaller angles of attack.

The flow in this case figure 6, forms a conical shock of varying strength; the windward side being stronger than the leeward. A pressure minimum develops about 30° from the leeward ray and an ever thickening boundary layer develops from the windward ray to this pressure minimum. Similarly, flow is drawn from the leeward ray towards the pressure minimum resulting in a thinner boundary layer on the leeward ray. The flow develops a recirculation vortex between the leeward ray and pressure minimum as the boundary layers from the windward and leeward side interact.

Several calculations for this case have been run; all of them at a Mach number of 4.25, Reynolds number per foot of 51.0E6., delta equal to 0.015, and streamwise step size varying from 0.002 to 0.02. Figure 6 shows the results of the last PEPSIS calculation for this case. The figure shows Mach number contours at a plane cutting through the axis of the cone. The conical shock is clearly visible as is the boundary layer structure along the cone surface. Qualitatively, the code correctly predicts the shock structure, the thickening boundary layer on the cone, the thinning of the boundary layer on the leeward side and the recirculation. Figure 7 shows details of this recirculation. The upper figure shows secondary velocity vectors and clearly indicates the recirculation in the s-shaped profiles near the top. Also evident are c-shaped profiles near the side which are also found experimentally. The lower figure shows Mach number contours in this region which again indicate a recirculation.

The calculation of figure 7 required an 80x50x220 (radial, circumferential, streamwise) mesh. The large number of mesh points were necessary to resolve all of the length scales for the important features of this flow problem; the creation of the conical shock, the movement of the shock away from the cone, the boundary layer and the recirculation region near the cone surface. Figure 8 demonstrates the importance of radial and circumferential mesh resolution for this problem. The figure shows Mach number contours for

the aft quadrant of the flow field for different meshes at a plane near the measuring station. All of the calculations required 220 streamwise stations, with nearly 100 of them located near the cone tip to resolve the formation of the shock. Figure 8(a) shows the results of the first calculation with 40 radial points packed near the cone surface and 19 circumferential points evenly spaced at every 10°. The results indicate a thickening of the boundary layer on the leeward side, and give no indication of a recirculation. Increasing the number of circumferential points to 37 evenly spaced at 5° while maintaing 40 radial points gives the results of figure 8(b). This calculation gives an indication of recirculation but with little detail. Because the recirculation is caused by interactions in the boundary layer, more resolution was required in the radial direction near the surface. Packing the 40 radial points closer to the surface, gave the results shown in figure 8(c). While resolving details of the surface, resolution of the shock wave was sacrificed which resulted in violent post shock pressure oscillations. To resolve both the shock and the boundary layer, the radial mesh was increased to 80 points. The results shown in figure 8(d) indicate that the calculation was then able to resolve boundary layer details without oscillations near the shock wave. Figure 8(e) shows one further refinement in which the circumferential mesh was increased to 50 points which were packed on both the windward and the leeward rays. The marked difference in the results of figure 8(a) and figure 8(e) clearly demonstrates the need to resolve all of the length scales present in this problem.

Figure 9 shows a quantitative comparison of circumferential static pressure distribution on the cone surface. The experimental values are given by the circles, while the results of a similarity analysis of Jones (ref. 11) are given by the squares. The comparison is very good, except near the windward ray, where the code underpredicts the pressure rise. There are several possible explanations for this discrepancy, including problems in the mixing length model near the plane of symmetry, errors in the mixing length scaling, or mesh resolution. A comparison of streamwise boundary layer profiles indicates that the calculated boundary layer thickness was too small for this test case. A thicker boundary layer would give a better agreement with experiment because the effective cone angle would be increased. The code does correctly model the pressure variations near the leeward ray.

Lewis 40-60 Inlet at Angle of Attack

One of the principal uses of the PEPSIS program will be the calculation of axisymmetric inlets at angle of attack. A verification test for this problem is presently planned at NASA Lewis using the 40-60 inlet. To demonstrate the code's ability to calculate inlets at angle of attack, the 40-60 inlet has been calculated at design Mach number at 2° angle of attack and at a Mach 3.0 overspeed at 2°. The design Mach number case failed due to subsonic flow on the leeward cowl at the first cowl reflection which qualitatively agrees with the results of an earlier wind tunnel test. The overspeed case was then calculated in order to better study the qualitative results of the code, and only results of this calculation are reported here.

For the inlet at design Mach number and at zero degrees angle of attack, the shock from the cone passes just off of the cowl lip. For the overspeed case, this shock is forced inside the cowl lip. At angle of attack, the shock translates forward on the leeward side and falls even farther inside on the windward side of the inlet creating a small expansion region on the cowl lip.

The calculation used a 49x19x480 mesh and wall function boundary conditions on solid surfaces. Considering the Rainbird results, boundary layer details for this rather coarse mesh are probably not resolved. However, the calculation does give the correct qualitative results for the inviscid part of the flow field. Figure 10 shows surface static pressure distribution on the cowl and cone. The shock waves are clearly shown as dark bands which are inclined relative to the inlet axis. On the cone, the shock system has moved forward on the leeward side and aft on the windward. On the cowl the first rather weak shock from the cone tip and the stronger shock from the cone reflection are evident. Also evident on the surface are pressure contours which are normal to the inlet axis, particularly near the throat section on the cone and along the cowl between shocks. These features are the results of compressions and expansions present in the inlet due to surface contouring. For another perspective, the plots of figure 11 show pressure and Mach number contours in the flow field at the windward, waterline, and leeward rays. On the windward ray, the cone shock falls inside the cowl; while on the leeward ray, the shock hits near the cowl lip. Pressure waves from the cowl contouring coalesce to strengthen the reflected shock more on the windward than the leeward. The reflected shock strikes the centerbody further forward on the leeward than the windward resulting in greater turning of the flow and a stronger shock on the leeward. For each shock reflection downstream of the throat, the leeward shock is stronger and has moved forward of the windward shock. Also evident are the expansions near the throat and its interaction with the shock system. Note that the expansion location is fixed geometrically while the shocks are not. The Mach number contours indicate this same behavior, but also shows the boundary layer variations through the calculation.

COMPUTING TIME

Because of the need to perform calculations on very large meshes, a premium is put on speed of the computer and the computer code. Table I documents the speed characteristics of the PEPSIS code on the NASA Lewis IBM 370 and CRAY I. There are two entries for the IBM 370 because the computer can be run in two basic modes; either debug, i.e., with an internal symbol dictionary (ISD), or in production (without ISD). The ISD imposes a performance penalty on the code which is documented in table I. The first two calculations were computed in the two-dimensional mode, and its speed advantage over the three-dimensional occurs as a result of keeping the whole problem in the core of the machine. The figures for the CRAY computer are estimates based on a seven to one speed increase over the IBM with ISD. A version of PEPSIS has been run on the CRAY to establish this ratio, although the version of the code used for this study has not yet been loaded on the CRAY at Lewis.

CONCLUSIONS

This paper has presented results from four test cases which are part of the verification effort for the three-dimensional supersonic inlet computer code PEPSIS. A two-dimensional calculation of the Lewis 40-60 axisymmetric mixed compression inlet indicated that the code qualitatively predicts the proper shock system formation. Wall static pressure distribution and boundary layer profiles fore and aft of a moderate bleed zone compared well with experimental results. The Rose test case verified the code's ability to quantitatively predict the details of an oblique shock-boundary layer interaction. The Rainbird test case of a 12.5° cone at angle of attack demonstrated the

code's ability to accurately model three-dimensional flow fields. The code has properly modeled the conical shock wave of varying strength, the cross flow boundary layer profiles and the leeward recirculation region. A large number of mesh points were required to resolve the details of all of these phenomenon; a mesh resolution study indicated that insufficient resolution gave either unstable or inaccurate results. Without a highly efficient, high speed code like PEPSIS, these detailed calculations would be impractical. The final test case involved the Lewis 40-60 inlet at 2° angle of attack. The results correctly model the three-dimensional shift of the shock system within axisymmetric inlets at angle of attack.

The calculation of supersonic inlet flow fields is an extremely complex problem because of the many flow phenomenon which occur. A typical axisymmetric inlet produces shock waves, expansions, boundary layers and their interaction with shock waves, and possible cross flow recirculations. For an accurate calculation, the computational mesh must resolve all of the length scales for all the phenomenon present in the flow. The Rainbird test case has illustrated possible problems associated with insufficient mesh resolution and indicated the magnitude of calculations which may be required for proper resolution.

In general, the PEPSIS code gave excellent results for the four test cases of this study. Although much work is planned to improve the fluid flow physics and decrease the computing time by conversion and optimization on the CRAY I computer, it is evident that the PEPSIS computer code is practical for three-dimensional supersonic inlet calculations.

REFERENCES

1. Buggeln, R.C., McDonald, H., Levy R., and Kreskovsky, J.P. "Development of a Three-Dimensional Supersonic Inlet Flow Analysis," NASA CR-3218, January, 1980.
2. Buggeln, R.C., McDonald H., and Kim, Y.N. "Computation of Multidimensional Viscous Supersonic Flow by Spatial Forward Marching," AIAA Paper No 83-0177, January 1983.
3. Anderson, B.H. and Towne, C.E., "Numerical Simulation of Supersonic Inlets Using a Three-Dimensional Viscous Flow Analysis," NASA TM-18411, January 1980.
4. Benson, T.J., "Application of Three Dimensional Viscous Marching Analysis to Supersonic Inlets," Advanced Computational Methods Workshop, NASA Lewis, November 1980.
5. Anderson, B.H., and Benson, T.J., "Numerical Solution to the Glancing Sidewall Oblique Shock Wave/Turbulent Boundary Layer Interaction in Three-Dimensions," AIAA Paper No 83-0136, January 1983.
6. Fukuda, M.K., Hingst, W.G., and Reshotko, E., "Control of Shock Wave-Boundary Layer Interactions by Bleed in Supersonic Mixed Compression Inlets," NASA CR-2595, August 1975.
7. Rose, W.C., "The Behavior of a Compressible Turbulent Boundary Layer in a Shock Wave Induced Adverse Pressure Gradient," PhD Thesis, University of Washington, 1972.
8. Rainbrd, W.J., "Turbulent Boundary Layer Growth and Separation on a Yawed Cone," AIAA Journal, December 1968, pp 2410,2416.
9. McDonald, H. and Camarata, F.J., "An Extended Mixing Length Approach for Computing the Turbulent Boundary Layer Development," Proceedings of Stanford Conference on Computation of Turbulent Boundary Layers Vol I, 1969, pp 83-98.

10. Maise, G. and McDonald, H., "Mixing Length and Kinematic Eddy Viscosity in a Compressible Boundary Layer," AIAA Journal, Vol 6, No 1, January 1968, pp 73–79.
11. Jones, D.J., "Numerical Solution of the Flow Field for Conical Bodies in a Supersonic Stream," NRCC Aeronautical Report LR 507, July 1968.

TABLE I - TEST CASES, MESH AND COMPUTING TIME

CASE	MESH	COMPUTING TIME (MIN)		
		IBM 370/3033		CRAY 1#
		ISD	NO ISD	
Lewis is 40-60 inlet at 0°	89x360 (32 040)	5.3	3.8	.7
Rose	89x450 (40 050)	6.6	4.7	.9
Rainbird	40x19x220 (167 200)	42.2	27.8	6.0
	80x50x220 (880 000)	----	144.4	31.7
Lewis 40-60 inlet at 0°	49x19x480 (446 880)	117.9	-----	16.8

#ESTIMATED TIME

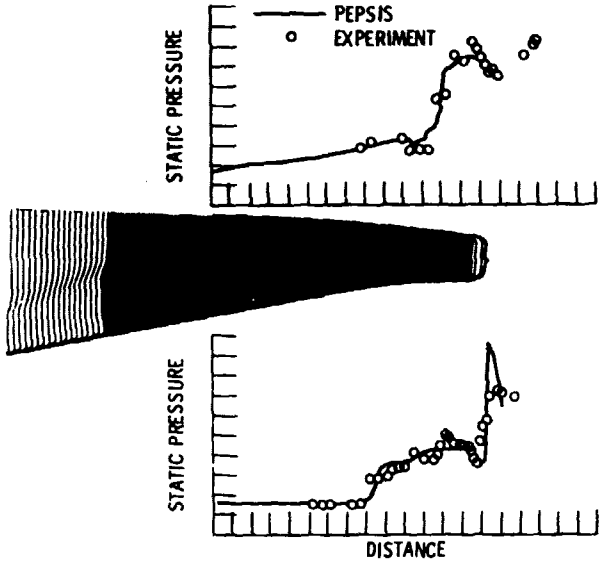

Figure 1. - Mach number profiles and wall static pressure distributions for Lewis 40-60 axisymmetric inlet.

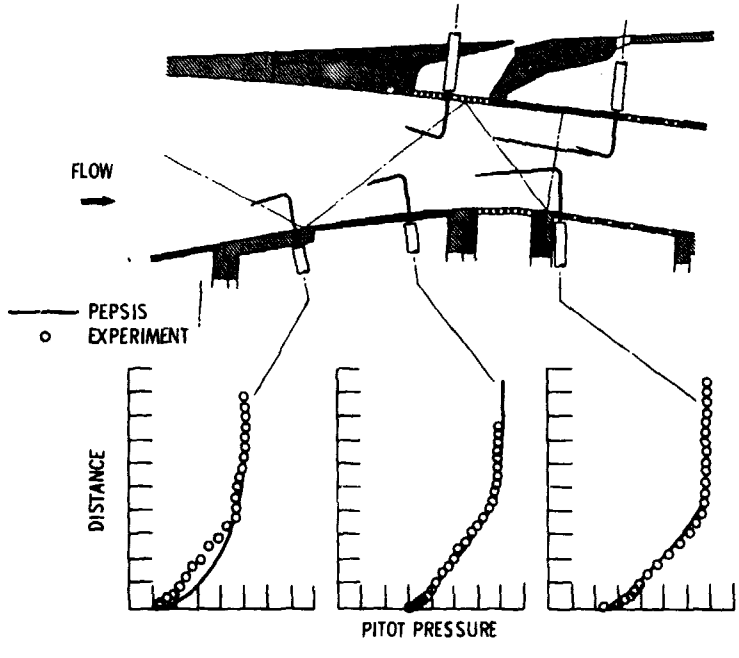

Figure 2. - Centerbody boundary layer profiles for Lewis 40-60 inlet.

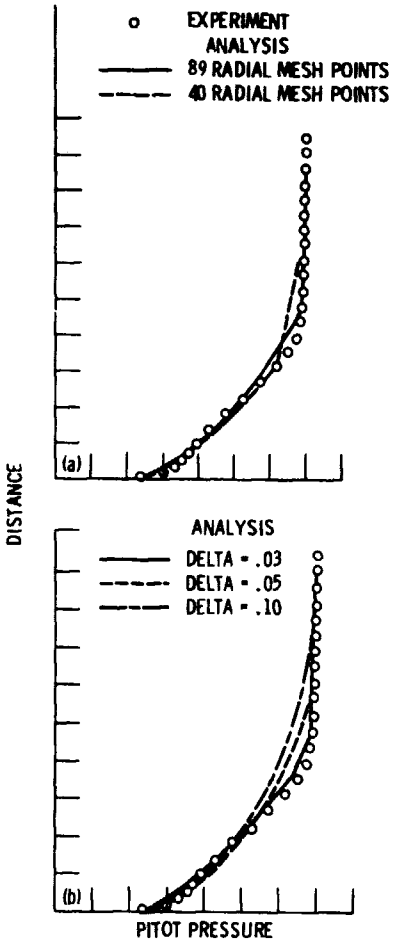

Figure 3. - Effects of input parameters on Lewis 40-60 inlet boundary layer profiles at rake 2.

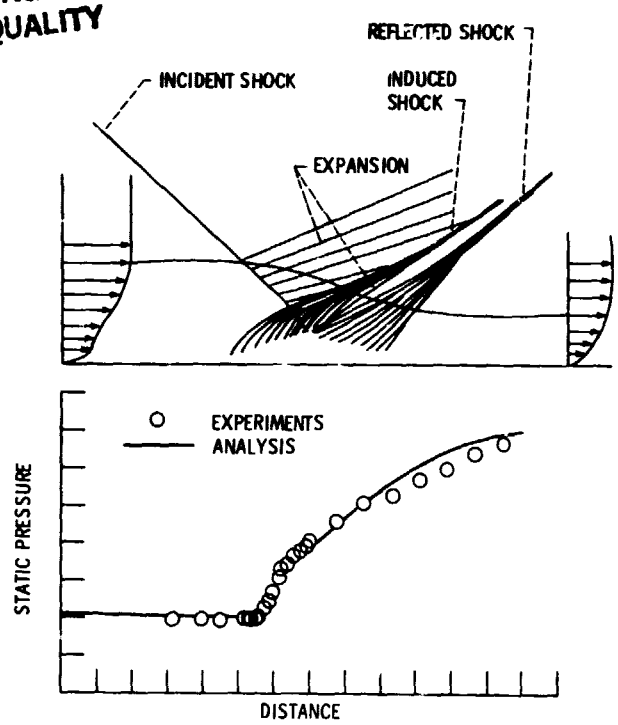

Figure 4. - Tunnel wall static pressure distribution for Rose shock-boundary layer interaction.

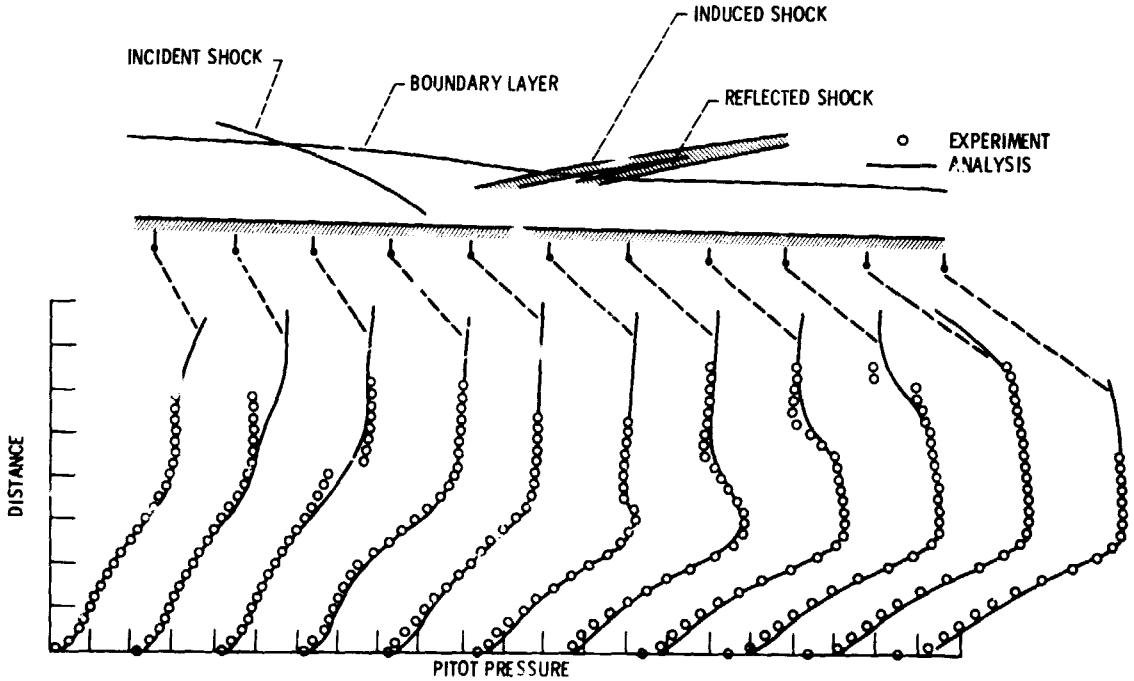

Figure 5. - Pitot pressure profiles for Rose shock-boundary layer interaction.

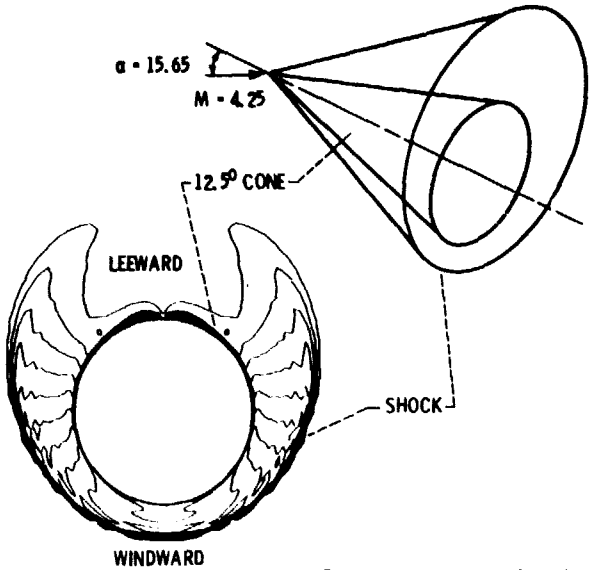

Figure 6. - Mach number contours for Rainbird cone at angle of attack.

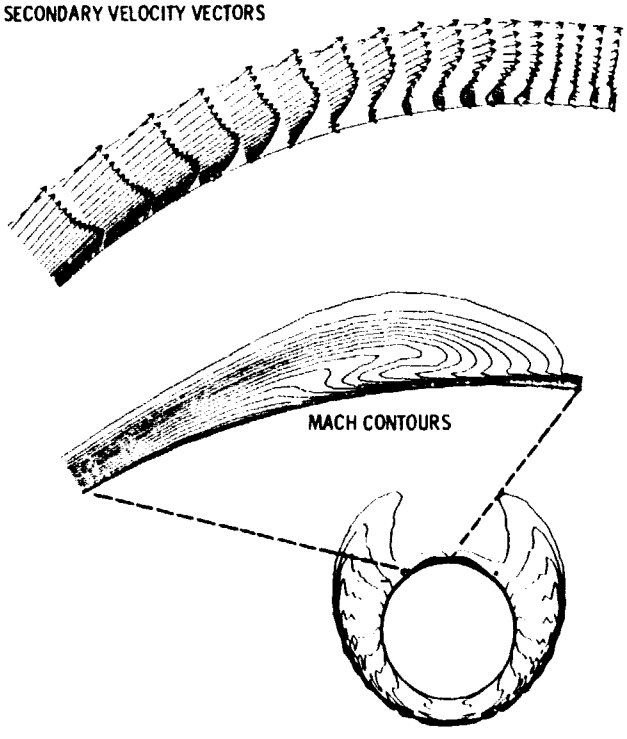

Figure 7. - Details of recirculation for Rainbird cone at angle of attack.

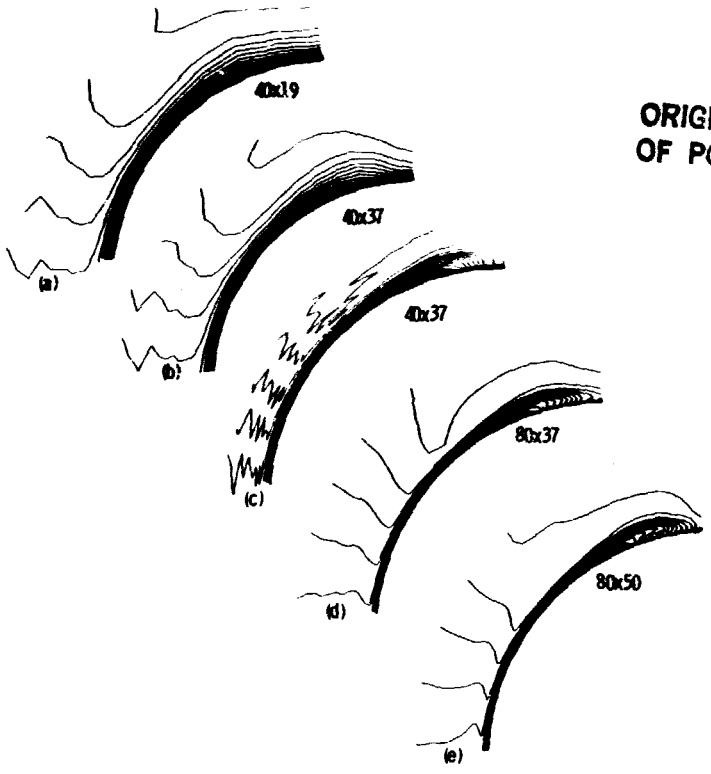

Figure 8. - Effects of mesh resolution on Rainbird cone at angle of attack.

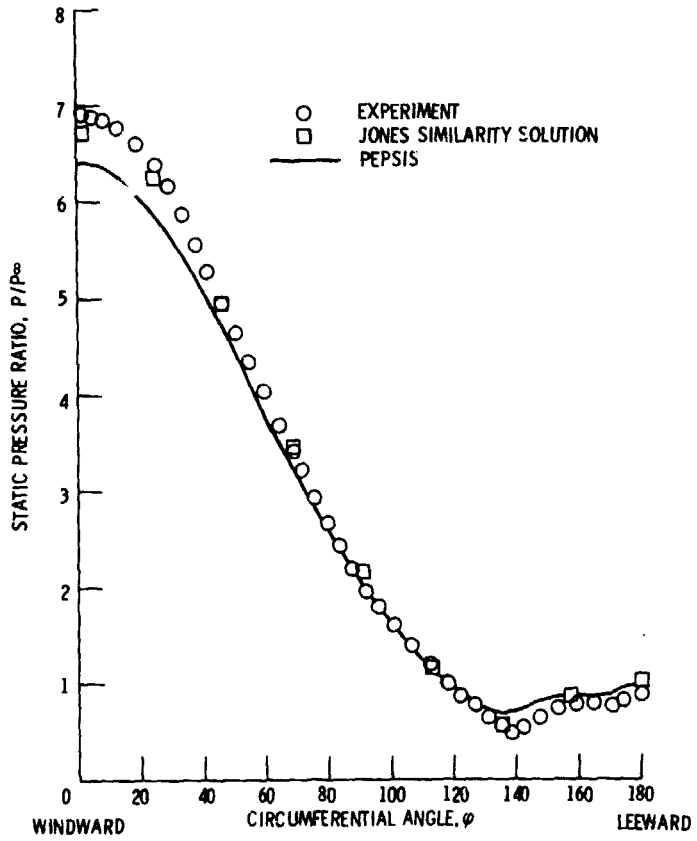

Figure 9. - Circumferential pressure distribution for Rainbird cone at angle of attack.

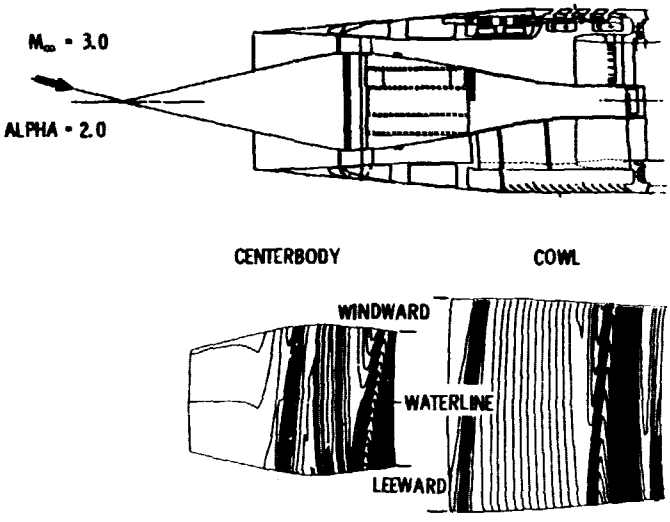

Figure 10. - Centerbody and cowl surface static pressure distribution for Lewis 40-60 inlet at angle of attack.

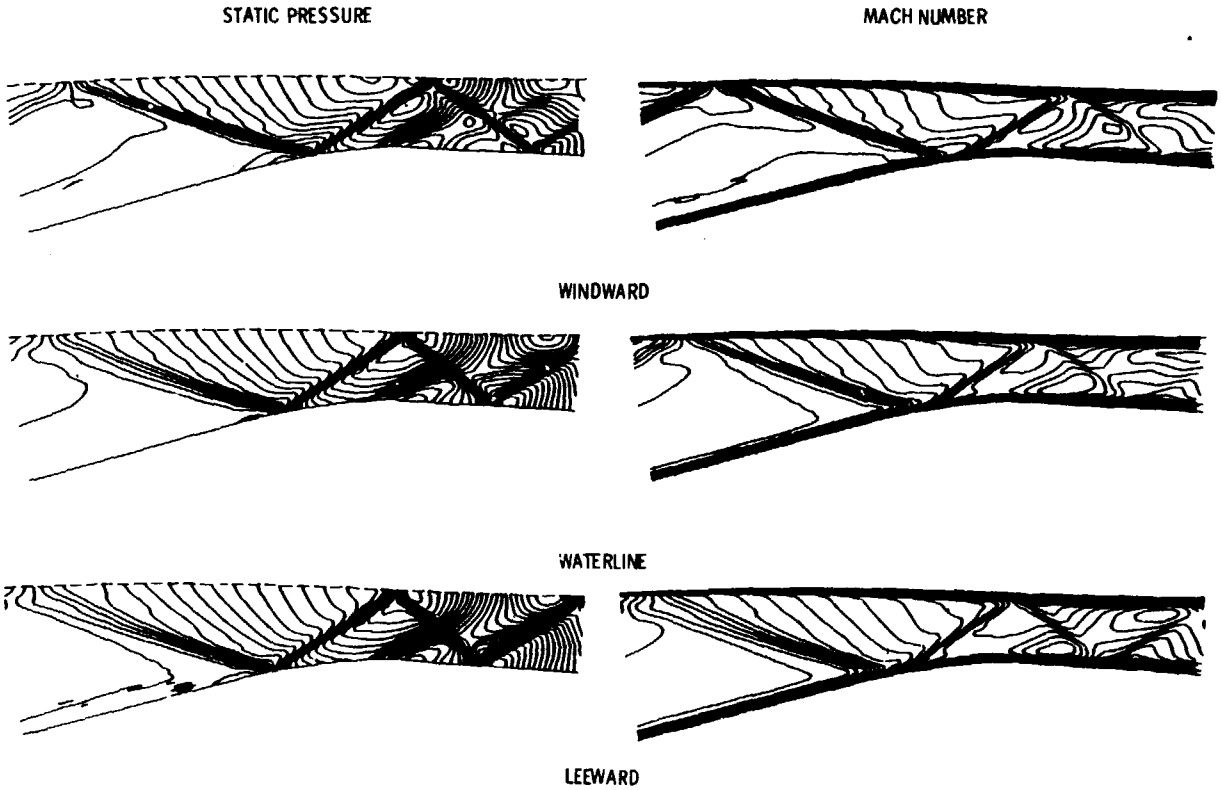

Figure 11. - Static pressure and Mach number contours for Lewis 40-60 inlet at angle of attack.